2021 IEEE International Conference on Robotics and Automation (ICRA 2021)
May 31 - June 4, 2021, Xi'an, China

The Effect of Input Signals Time-Delay on Stabilizing Traffic with Autonomous Vehicles

Isam Al-Darabsah, Mohammad Al Janaideh, and Sue Ann Campbell

Abstract— **This paper extends the results in [1] considering time delays in Standard Car Following models (CFMs). In [1], connected vehicles are characterized with CFMs models and controlled using linear string analysis to stabilize single-lane car following of human-driven vehicles (HDVs). In this paper, we revisit stability and safety conditions for traffic considering time delays due to lags in the input signals. We perform plant stability and string stability analysis to derive these conditions. Then we obtain the optimal number of HDVs that can be stabilized using one autonomous vehicle. Numerical simulations are provided to implement a case study on Intelligent Driver Model to discuss the influence of time delays that arise on HDVs and the autonomous vehicle on optimal number of HDVs that can be stabilized using one autonomous vehicle.**

I. INTRODUCTION

Traffic jams are growing in metropolitan areas and it is expected to increase in the future. Usually, traffic congestion leads to stop-and-go waves within human-driven vehicles (HDVs), which increase fuel consumption, and affect traffic safety and flow [2]. This is related to the concept of *string instability*, where a perturbation of the flow equilibrium causes amplifies the spacing errors downstream of the traffic flow [3]. Different Car Following Models (CFMs) have been used to simulate road traffic. For example, the Intelligent Driver Model (IDM) is used to evaluate human behavior and to implement adaptive cruise control [4].

In order to reduce traffic jams, a number of techniques have been used to optimize driving efficiency and safety for the individual controlled vehicles. In [1], a single autonomous vehicle is proposed to dampen the stop and go waves and to mitigate traffic jams of HDVs. The study shows that a single autonomous vehicle can manage future transportation to have traffic flow without traffic jams. In [5], experimental results show that an autonomous vehicle with intelligent control techniques can dampen stop-and-go waves of of twenty HDVs on a ring road and decrease fuel consumption. In [6], traffic flow on a ring with a single autonomous Vehicle is studied. Other studies propose deep learning approaches to enhance the dissipation of the stop-and-go waves, see, e.g., [7].

Time delays can change the dynamics of vehicle network and lead to faulty control signals. There are different sources for time delays. For instance, in [8], the authors study CFM with a time delay to represent the driver's reaction time. In [9], the authors incorporate time delays in communication-based controller design in connected vehicle networks, which arise due to digital implementation and intermittent vehicle-to-vehicle communication. In [10], the authors propose a vehicle model and design a controller based on the information received via wireless connection with stochastic delay subject to stochastic packet drops.

The goal of this work is to extend the results in [1], considering time delays that arise from lags in the input signals. More precisely, we use one autonomous vehicle to prevent string instability of the system of human-driven vehicles and make the system string stable, which prevents the formation of traffic jams. The contributions of this paper are (i) Provide plant stability and string stability analyses for a linear system corresponding to a time-delayed Standard Car Following model, (ii) Obtain the maximal admissible delay region such that the time-delayed system remains plant stable, (iii) Derive stability and safety conditions and obtain the optimal number of HDVs that can be stabilized using one autonomous vehicle, and (iv) Conduct numerical simulation to apply the results to Intelligent Driver Model.

The rest of the paper is organized as follows: First, we introduce a general nonlinear time-delayed CFM and its corresponding linear system at the flow equilibrium in Section II. Then, in Section III, we carry out plant stability analysis and provide a range of time delay in which the system is plant stable. In Section IV, we provide stability and safety conditions through a string stability analysis. Then, we use these conditions to characterize the optimal number of HDVs that can be stabilized by one autonomous vehicle. Section Section V presents the numerical simulation using an intelligent Driver Model. We discuss the effects of time delays that arise in HDVs and the autonomous vehicle on the optimal number of HDVs that can be stabilized using one autonomous vehicle. Section VI concludes the paper.

II. TIME-DELAYED CAR FOLLOWING MODEL

Consider $n+1$ vehicles in single-lane road. We assume that each vehicle i obeys a time-delayed *car following model* (CFM) of the form

$$a_i(t) = \dot{v}_i(t) = f\big(h_i(t-\epsilon_i), \dot{h}_i(t-\epsilon_i), v_i(t-\epsilon_i)\big), \quad i = 0, 1, \ldots, n, \tag{1}$$

where a_i is acceleration, h_i the headway distance, $\dot{h}_i$ the headway relative velocity, and v_i is the velocity.The time delay ϵ_i represents the delay of the input signals h_i, $\dot{h}_i$, v_i to the resulting output acceleration a_i. The CFMs include

I. Al-Darabsah and S. A. Campbell are with the Department of Applied Mathematics at University of Waterloo, Waterloo, ON, N2L 3G1, Canada. Email: ialdarabsah@gmail.com, sacampbell@uwaterloo.ca. M. Al Janaideh is with the Department of Mechanical Engineering, Memorial University, St. John's, NL, A1B 3X5, Canada. Email: maljanaideh@mun.ca.

978-1-7281-9077-8/21/$31.00 ©2021 IEEE

the Optimal Velocity Model (OVM) [11] and the Intelligent Driver Model (IDM) [12].

In the literature, platooning cars are said to be in *uniform flow equilibrium* when each car moves at a constant velocity of v^* with constant headway h^*. Then the uniform flow equilibrium satisfies

$$a_i = f\big(h^*, 0, v^*\big) = 0. \tag{2}$$

To characterize the dynamics of system (1), we study the linear system corresponding to the flow equilibrium. The linearization of (1) about the flow equilibrium is

$$\begin{aligned} a_i(t) = k_p\left(h_i(t-\epsilon_i) - h^*\right) + k_d \dot{h}_i(t-\epsilon_i) \\ + k_v\left(v_i(t-\epsilon_i) - v^*\right) \end{aligned} \tag{3}$$

where k_p, k_d and k_v are constants and can be obtained as

$$\begin{aligned} &k_p = f_1(h^*, 0, v^*), \quad k_d = f_2(h^*, 0, v^*), \\ &k_v = f_3(h^*, 0, v^*), \end{aligned} \tag{4}$$

where f_j, $j = 1, 2, 3$, is the derivative of f with respect to its j-th argument. Denote $\hat{x}_i(t)$ to be the absolute position of vehicle i at time t and $x_i(t)$ to be the position of vehicle i relative to its flow equilibrium at time t. Now we write system (3) in terms of x_i and transform it into a suitable form. For $i \in \{1, \ldots, n\}$, let

$$\hat{h}_i(t) := \hat{x}_{i-1}(t) - \hat{x}_i(t), \tag{5}$$

$$x_i(t) := \hat{x}_i(t) + ih^* - tv^*. \tag{6}$$

Then, (3) can be written as

$$\begin{aligned} \ddot{x}_i(t) =& k_p\left(x_{i-1}(t-\epsilon_i) - x_i(t-\epsilon_i)\right) \\ &+ k_d\left(\dot{x}_{i-1}(t-\epsilon_i) - \dot{x}_i(t-\epsilon_i)\right) - k_v \dot{x}_i(t-\epsilon_i). \end{aligned} \tag{7}$$

In this work, we obtain the plant stability and string stability of (7).

III. Stability Analysis

A vehicle network is said to be plant stable when the leading vehicle moves with a constant speed, perturbations in the states of following vehicles approach zero, that is, when $\dot{x}_0(t) \equiv 0$, then $\dot{x}_i(t) \to 0$ as $t \to \infty$ for $i = 1, \ldots, n$ [13]. This is equivalent to the zero solution of (7) being stable, that is, the real part of all eigenvalues of the characteristic equation is negative.

The stability of (7) is determined by the sign of the real part of the eigenvalues of its corresponding characteristic equation. Let

$$x(t) = \mathbf{C}\mathrm{e}^{\lambda t}, \ \lambda \in \mathbb{R}, \ \mathbf{C} \in \mathbb{R}^n. \tag{8}$$

Then, the characteristic equation associated with (7) has the form

$$\Delta(\lambda) := \begin{vmatrix} \mathbf{A}_1 & \mathbf{0} & \mathbf{0} & \mathbf{0} & \cdots & \mathbf{0} \\ \mathbf{B}_2 & \mathbf{A}_2 & \mathbf{0} & \mathbf{0} & \cdots & \mathbf{0} \\ \mathbf{0} & \mathbf{B}_3 & \mathbf{A}_3 & \mathbf{0} & \cdots & \mathbf{0} \\ \mathbf{0} & \mathbf{0} & \mathbf{B}_4 & \mathbf{A}_4 & \mathbf{0} & \vdots \\ \vdots & \vdots & \ddots & \ddots & \ddots & \mathbf{0} \\ \mathbf{0} & \mathbf{0} & \cdots & \mathbf{0} & \mathbf{B}_n & \mathbf{A}_n \end{vmatrix} = 0 \tag{9}$$

where

$$\mathbf{A}_i = \begin{bmatrix} \lambda & -1 \\ k_p \mathrm{e}^{-\lambda\epsilon_i} & \lambda + (k_d + k_v)\,\mathrm{e}^{-\lambda\epsilon_i} \end{bmatrix}$$

and

$$\mathbf{B}_i = \begin{bmatrix} 0 & 0 \\ -k_p \mathrm{e}^{-\lambda\epsilon_i} & -k_d \mathrm{e}^{-\lambda\epsilon_i} \end{bmatrix}.$$

By [14, Proposition 2.7.1], we obtain that

$$\Delta(\lambda) = \prod_{i=1}^{n} \det\left(\mathbf{A}_i\right) = 0, \tag{10}$$

with

$$\det\left(\mathbf{A}_i\right) = \lambda^2 + (k_d + k_v)\,\mathrm{e}^{-\lambda\epsilon_i}\lambda + k_p \mathrm{e}^{-\lambda\epsilon_i}. \tag{11}$$

Thus, for some $i \in \{1, 2, \ldots, n\}$

$$\Delta(\lambda) = 0 \Leftrightarrow \det\left(\mathbf{A}_i\right) = 0.$$

For $i = 1, \ldots, n$, if $\det\left(\mathbf{A}_i\right) = 0$ has a root with a positive real part, then so does (9). Consequently, we have:

Lemma 3.1: If $k_p < 0$, then the zero solution of (7) is unstable.

Proof: In (11), it is clear that $\det\left(\mathbf{A}_i\right)|_{\lambda=0} = k_p$ and $\lim\limits_{\lambda\to\infty} \det\left(\mathbf{A}_i\right) \to \infty$. Thus, the equation (9) has a positive real root when $k_p < 0$. Thus, $x(t) \to \infty$ as $t \to \infty$, and hence, the zero solution is unstable. ■

From Lemma 3.1, we assume that $k_p \geq 0$ in the rest of the section. To construct the maximal admissible delay region such that the time-delayed system remains stable, first, we study the case When there is no delay ($\epsilon_i = 0$) in the model (7). In this case, we have

$$\det\left(\mathbf{A}_i\right) = \lambda^2 + \left(k_d + k_v\right)\lambda + k_p. \tag{12}$$

Then, by the Routh-Hurwitz stability criterion [15], we have

Lemma 3.2: When $\epsilon_i = 0$ for all $i \in \{1, \ldots, n\}$, the zero solution of (7) is stable if and only if

$$k_d + k_v > 0 \quad \text{and} \quad k_p > 0. \tag{13}$$

The condition (13) is physically reasonable and reflects the real driving behavior [16].

Now, let $\epsilon_i > 0$, it is clear that, $\lambda = 0$ is an eigenvalue of (9) if and only if $k_p = 0$. Assume $k_p > 0$ and suppose $\lambda = j\eta$ ($\eta > 0$ and $j = \sqrt{-1}$) is a purely imaginary eigenvalue of $\det(\mathbf{A}_i) = 0$. By separating the real and imaginary parts, we obtain:

$$\eta^2 = (k_d + k_v)\eta\sin(\eta\epsilon_i) + k_p\cos(\eta\epsilon_i), \tag{14}$$

$$0 = (k_d + k_v)\eta\cos(\eta\epsilon_i) - k_p\sin(\eta\epsilon_i). \tag{15}$$

Squaring and adding the above equations lead to

$$\Xi\left(\xi\right) := \xi^2 - (k_d + k_v)^2\xi - k_p^2 = 0, \tag{16}$$

where $\xi = \eta^2$. Notice that $(k_d + k_v)^2 + 4k_p^2 > 0$, $-(k_d + k_v)^2 < 0$ and $\xi\left(0\right) = -k_p^2 \leq 0$. Hence, Ξ has exactly one positive root. Thus,

$$\eta_0 = \left(\frac{(k_d + k_v)^2 + \sqrt{(k_d + k_v)^4 + 4k_p^2}}{2} \right)^{\frac{1}{2}}. \quad (17)$$

Plugging $\eta = \eta_0$ into (14)-(15) and solving the resulting equation for $\cos(\eta_0 \epsilon_i)$ and $\sin(\eta_0 \epsilon_i)$ leads to

$$\cos(\eta_0 \epsilon_i) = \frac{k_p \eta_0^2}{(k_d + k_v)^2 \eta_0^2 + k_p^2} := P_0$$

and

$$\sin(\eta_0 \epsilon_i) = \frac{(k_d + k_v)\eta_0^3}{(k_d + k_v)^2 \eta_0^2 + k_p^2} := Q_0.$$

Since η_0, P_0 and Q_0 are independent of car i, we obtain a sequence of critical values for the delay parameter

$$\hat{\epsilon}_k = \frac{1}{\eta_0} \arccos\left(\frac{k_p \eta_0^2}{(k_d + k_v)^2 \eta_0^2 + k_p^2} \right) + \frac{2k\pi}{\eta_0},\ k \in \mathbb{Z}_0^+. \quad (18)$$

when $Q_0 > 0$ and

$$\hat{\epsilon}_k = \frac{1}{\eta_0} \left[2\pi - \arccos\left(\frac{k_p \eta_0^2}{(k_d + k_v)^2 \eta_0^2 + k_p^2} \right) \right] + \frac{2k\pi}{\eta_0},\ k \in \mathbb{Z}_0^+ \quad (19)$$

when $Q_0 < 0$. Here, $\mathbb{Z}_0^+ = \{0, 1, \ldots\}$. We now have the following result.

Theorem 3.1: At each critical value $\hat{\epsilon}_k$ defined in (18),

$$\operatorname{sign}\left\{ \frac{d(\operatorname{Re}\{\lambda(\epsilon_i)\})}{d\epsilon_i} \bigg|_{\epsilon_i = \hat{\epsilon}_k} \right\} > 0. \quad (20)$$

Proof: Taking the derivative of $\det(\mathbf{A}_i)|_{\lambda = \lambda(\epsilon_i)} = 0$ with respect to ϵ_i leads to

$$\left(\frac{d\lambda(\epsilon_i)}{d\epsilon_i} \right)^{-1} = \frac{2\lambda(\epsilon_i) \mathrm{e}^{\lambda(\epsilon_i)\epsilon_i} - (k_d + k_v)}{\lambda(\epsilon_i)((k_d + k_v)\lambda(\epsilon_i) + k_p)} - \frac{\epsilon_i}{\lambda(\epsilon_i)}. \quad (21)$$

Notice that when $\epsilon_i = \hat{\epsilon}_k$, (9) has a pure imaginary root $\lambda(\epsilon_i) = j\eta$. Hence, by using (14), we have

$$\operatorname{Re}\left(\frac{d\lambda(\epsilon_i)}{d\epsilon_i} \right)^{-1} \Bigg|_{\epsilon_i = \hat{\epsilon}_k} = \frac{(k_d + k_v)^2 + 2\eta^2}{(k_d + k_v)^2 \eta^2 + k_p^2} > 0. \quad (22)$$

The result follows from

$$\operatorname{sign}\left\{ \frac{d(\operatorname{Re}\{\lambda(\epsilon_i)\})}{d\epsilon_i} \bigg|_{\epsilon_i = \hat{\epsilon}_k} \right\} = \operatorname{sign}\left\{ \operatorname{Re}\left(\frac{d\lambda(\epsilon_i)}{d\epsilon_i} \right)^{-1} \Bigg|_{\epsilon_i = \hat{\epsilon}_k} \right\} > 0.$$

■

Theorem 3.1 implies that the eigenvalue $\lambda(\epsilon_i)$ crosses the imaginary axis from left to right in a neighborhood of $\epsilon_i = \hat{\epsilon}_k$, $k \in \mathbb{Z}_0^+$. Indeed (20) is called "the transversality\crossing condition" due to the positive speed of the eigenvalues when they cross the imaginary axis. Hence, at these critical time delay value, a stable solution becomes unstable. The following result is straightforward from Theorem 3.1 and Lemma 3.2.

Theorem 3.2: Assume $k_d + k_v > 0$ and $k_p > 0$ such that the zero solution of (7) is stable when $\epsilon_i = 0$. Then, it remains stable for $\epsilon_i \in (0, \epsilon^*)$ and becomes unstable for $\epsilon_i > \epsilon^*$ where

$$\epsilon^* = \min\left\{ \hat{\epsilon}_k : k \in \mathbb{Z}_0^+ \right\}. \quad (23)$$

Theorem 3.2 implies that all eigenvalues of (10) are negative when $\epsilon \in (0, \epsilon^*)$, thus the exponential terms in (8) will go to zero as $t \to \infty$. Hence, $\dot{x}(t)$ in (7) goes to zero as $t \to \infty$, that is, the system is plant stable. Furthermore, the system is plant unstable when at least one delay exceeds ϵ^*.

Remark 3.1: It is clear that ϵ^* is independent of car i, and hence, it can be calculated from (17)-(19) with the values in (4).

IV. String stability Analysis

In this section, we study the string stability of (7) in the presence of time delays. This is critical in the dynamics of the vehicle network to avoid amplifying the spacing errors downstream of the traffic flow [17]. The string instability of a platoon of vehicles can cause the emergence of a jam, such as stop and go, in circuits and single-lane roads. Through this section, we consider the following assumptions as in [1]: (i) HDVs models are homogeneous and have the same vehicle dynamics, (ii) HDVs models are string unstable in some traffic conditions; and (iii) All vehicle models are plant stable, that it, $\epsilon_i \in (0, \epsilon^*)$.

Denote $T_i(s)$ to be the transfer function of the linear dynamics in (7) assuming zero initial condition. Then, for vehicle i:

$$T_i(s) := \frac{X_i(s)}{X_{i-1}(s)} = \frac{(sk_d + k_p)\mathrm{e}^{-s\epsilon_i}}{s^2 + (k_d + k_v)s\mathrm{e}^{-s\epsilon_i} + k_p \mathrm{e}^{-s\epsilon_i}} \quad (24)$$

where $X(s)$ is the Laplace transform of $x(t)$.

Definition 4.1 (Vehicular string stability [1]): A vehicle with transfer function $T(\cdot)$ is string stable if and only if $|T(j\omega)| \leq 1$ for all ω. Equivalently, $\|T(j\omega)\|_\infty \leq 1$.

Let $s = j\omega$, $\omega \in \mathbb{R}^+$, then for each vehicle i, the string stability holds if $|T_i(j\omega)| \leq 1$ for $i = 1, \ldots, n$ [18]. It follows from (24) that

$$|T_i(j\omega)|^2 = \frac{p}{p + q}$$

where $p = k_p^2 + k_d^2 \omega^2 \geq 0$ and

$$q = \omega^4 + (2k_d k_v + k_v^2)\omega^2 - 2(k_d + k_v)\omega^3 \sin(\epsilon_i \omega) - 2k_p \omega^2 \cos(\epsilon_i \omega).$$

Since $p \geq 0$, it is clear that $|T_i(j\omega)| \leq 1$ when $q \geq 0$. Assume

$$k_d + k_v > 0 \quad \text{and} \quad k_p > 0. \quad (25)$$

Notice that the condition (25) is similar to the one in Lemma 3.2 and it reflects the real driving behavior [16]. Then, it follows from $\cos(\epsilon_i \omega) \leq 1$ and $\sin(\epsilon_i \omega) \leq \epsilon_i \omega$ that

$$q \geq \left[1 - 2\epsilon_i (k_d + k_v) \right] \omega^4 + (2k_d k_v + k_v^2 - 2k_p)\omega^2.$$

It is clear that $q \geq 0$ if

$$\omega \geq \sqrt{\frac{2k_p - 2k_d k_v - k_v^2}{1 - 2\epsilon_i(k_d + k_v)}} := \hat{\omega}(\epsilon_i). \tag{26}$$

provided $2k_d k_v + k_v^2 \leq 2k_p$ and

$$0 < \epsilon_i < \frac{1}{2(k_d + k_v)} := \hat{\epsilon}. \tag{27}$$

In (26), notice that we omit condition $2\epsilon_i(k_d + k_v) > 1$ since it does not hold at $\epsilon_i = 0$. It is clear that

$$\frac{d\hat{\omega}(\epsilon_i)}{d\epsilon_i} = \frac{k_v + k_d}{1 - 2\epsilon_i(k_d + k_v)}\hat{\omega}(\epsilon_i) > 0.$$

Consequently, we have the following result.

Theorem 4.1: Assume $\epsilon_i < \hat{\epsilon}$ for all $1, \ldots, n$ and let $\epsilon_{\max} = \max\{\epsilon_i : i = 1, \ldots, n\}$. Then, the linear HDVs model (k_p, k_d, k_v) (3) is string stable if $\omega \geq \omega_0$ where $\omega_0 = \hat{\omega}(\epsilon_{\max})$.

It follows from Theorem 4.1 that the linear HDVs model can be string unstable only if $\omega \in (0, \omega_0)$.

Lemma 4.1: For each car, the range of frequencies $(0, \omega_0)$ becomes bigger as the time delay ϵ_i increases.

In [1], the authors studied the sting stability of (1) without time delays. In this case, $\omega_0 = \sqrt{2k_p - 2k_d k_v - k_v^2}$. Comparing (4.1) to the result in [1], we find that existence of ω_0 is affected by presence of the time delays. The region of existence of ω_0 in (k_p, k_v, k_d)-space becomes smaller as ϵ increases, see Fig. 1.

Now we study the string stability of a lane traffic system of m HDVs and a single autonomous vehicle. We denote the transfer function of "human car following model" by $T_H(s)$ and the transfer function of "autonomous vehicle controller" by $T_R(s)$ where, for $\sigma \in \{H, R\}$,

$$T_\sigma(s) := \frac{(sk_{d_\sigma} + k_{p_\sigma})\mathrm{e}^{-s\epsilon_\sigma}}{s^2 + (k_{d_\sigma} + k_{v_\sigma})s\mathrm{e}^{-s\epsilon_\sigma} + k_{p_\sigma}\mathrm{e}^{-s\epsilon_\sigma}}. \tag{28}$$

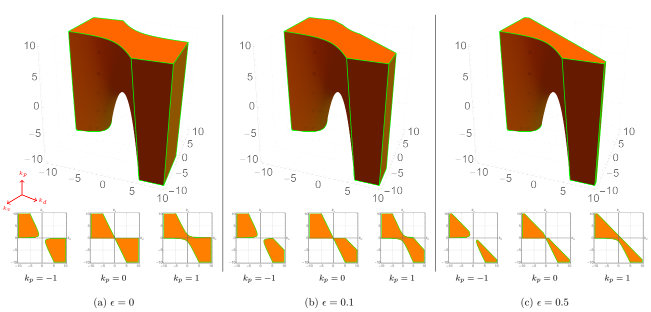

Fig. 1. Illustration of the region of ω_0 existence in (k_p, k_v, k_d)-space (k_v, k_d)-plane.

Definition 4.2 (System-level string stability [1]): Let $\{T_i(\cdot)\}_{i=1}^N$ denote the transfer functions of the N vehicles in a single lane traffic system. This system is string stable if and only if

$$\left\| \prod_{i=1}^{N} T_i(j\omega) \right\|_\infty \leq 1. \tag{29}$$

Notice that the length of the string is omitted in Definition 4.2. The following result gives the maximum number of HDVs that can be stabilized under any input disturbance by a given autonomous car controller.

Theorem 4.2: Consider a string of an m string unstable HDVs followed by a single autonomous vehicle. Then, the maximum number of vehicles that can be string stabilized is given by

$$m^*_{\text{stable}} = \left\lfloor \min_{\omega \in (0,\omega_0)} \{F_{\text{stable}}(\omega)\} \right\rfloor \tag{30}$$

with

$$F_{\text{stable}}(\omega) = -\frac{\log|T_R(j\omega)|}{\log|T_H(j\omega)|} \tag{31}$$

where $\lfloor \cdot \rfloor$ is the floor function.

Proof: First, notice that the order of the vehicles does not matter due to the linearity of the scalar systems. Let $x_R(t)$ be the position of the autonomous vehicle (relative to its flow equilibrium position) and $X_R(s)$ be its Laplace transform. Now, assume that the behavior of the leading HDV is governed by its reaction to some input (disturbance) $d(t)$. Then, from (24), we have

$$X_R(s) = T_R(s)\Big(T_H(s)\Big)^m D(s), \tag{32}$$

where $D(s)$ is the Laplace transform of $d(t)$. By Definition 4.2, the system is string stable if it attenuates all unstable disturbances, that is, for $s = j\omega$ and $\omega \in (0, \omega_0)$:

$$\begin{aligned} &|T_R(j\omega)(T_H(j\omega))^m| \leq 1 \\ &\qquad \Leftrightarrow \log|T_R(j\omega)| + m\log|T_H(j\omega)| \leq 0 \\ &\qquad \Leftrightarrow m \leq -\frac{\log|T_R(j\omega)|}{\log|T_H(j\omega)|} \end{aligned} \tag{33}$$

Since (33) holds for all $\omega \in (0, \omega_0)$. Then,

$$m \leq \min_{\omega \in (0,\omega_0)} \left\{ -\frac{\log|T_R(j\omega)|}{\log|T_H(j\omega)|} \right\}. \tag{34}$$

It is clear that m is an integer, and hence, we have m^*_{stable} in (30).

■

Remark 4.1: Outside the range $(0, \omega_0)$, the system described in Theorem 4.2 is string stable due to $\|T(j\omega)\|_\infty \leq 1$ for all cars and (29) is straightforward satisfied.

Since the string stability as defined in Definition 4.2 does not prohibit collisions between vehicles or inefficient driving behavior [1], we add *headway bounds* on $h(t)$ to ensure safety by maintaining separation between vehicles.

Definition 4.3 (Headway bounds [1]): The *safety bound* $\Lambda_- > 0$ is the minimum headway that a vehicle is allowed to experience regardless of any given external disturbance:

$$h(t) > \Lambda_- \qquad \forall t > 0. \tag{35}$$

On the other hand, the *performance bound* is the maximum allowable headway $\Lambda_+ > 0$ that a vehicle can permit:

$$h(t) < \Lambda_+ \qquad \forall t > 0. \tag{36}$$

The *headway bound* $\Lambda \in (0, h^*)$ satisfies

$$h^* - \Lambda < h(t) < h^* + \Lambda \qquad \forall t > 0. \tag{37}$$

For a given $\Lambda \in (0, h^*)$ we can choose $\Lambda_- = h^* - \Lambda$ and $\Lambda_+ = h^* + \Lambda$. Notice Λ_- guarantees safety by maintaining separation between vehicles and Λ_- guarantees that the vehicle does not lag too far behind the rest of the traffic.

The following result gives a safety condition when there is an oscillatory or impulse disturbance.

Theorem 4.3: For a given disturbance $d(t) = \beta u(t)$ and headway bound Λ, the maximum number of vehicles a single autonomous vehicle can safely and efficiently follow is given by

$$m^*_{\text{safe}} = \left\lfloor \min_{\omega \in (0,\omega_0)} \left\{ \frac{\log \zeta - \log|1 - T_R(j\omega)|}{\log|T_H(j\omega)|} \right. \right. \\ \left. \left. - \frac{\log|U(j\omega)| + \log(j\omega)}{\log|T_H(j\omega)|} \right\} \right\rfloor \tag{38}$$

where $\zeta := \frac{\Lambda}{\beta}$ and $U(s)$ is the Laplace transform of $u(t)$.

Proof: Let $x_F(t)$ be the position of the final HDV in the string. Then, its Laplace transform is

$$X_F(s) = \Big(T_H(s)\Big)^m D(s), \tag{39}$$

giving rise to the headway experienced by the autonomous vehicle

$$h_R(t) - h^* = x_N(t) - x_R(t). \tag{40}$$

From (32) and (39), we have

$$X_N(s) - X_R(s) = \beta (T_H(s))^m \left(1 - T_R(s)\right) U(s). \tag{41}$$

From 40 and Definition 4.3, we have

$$\beta \left|(T_H(s))^m \left(1 - T_R(s)\right) U(s)\right| < \frac{\Lambda}{s}$$

Let $\zeta := \frac{\Lambda}{\beta}$. Then,

$$m \log|T_H(s)| + \log|1 - T_R(s)| + \log|U(s)| < \log\frac{\zeta}{s}.$$

Thus,

$$m < \frac{\log \zeta - \log|1 - T_R(s)| - \log|U(s)| - \log s}{\log|T_H(s)|}.$$

Notice that m is integer. Then, for $s = j\omega$ and $\omega \in (0, \omega_0)$, we have m^*_{safe} in (38). ■

Lemma 4.2: When there is step disturbance $d(t) = \beta$ in Theorem 4.3. Then,

$$m^*_{\text{safe}} = \left\lfloor \min_{\omega \in (0,\omega_0)} \{F_{\text{safe}}(\omega)\} \right\rfloor \tag{42}$$

with

$$F_{\text{safe}}(\omega) = \frac{\log \zeta - \log|1 - T_R(j\omega)|}{\log|T_H(j\omega)|}. \tag{43}$$

Combining Theorem 4.2 and Lemma 4.2 when $d(t) = \beta$, we optimize a linear HDV model T_H and safety parameter ζ by taking

$$m^* = \max_{T_R} \min\{m^*_{\text{stable}}, m^*_{\text{safe}}\}. \tag{44}$$

as in [1] which represents the maximum number of HDVs that can stabilize, safely and efficiently.

V. Numerical Results

In this section, we consider a human Intelligent Driver Model (IDM) driver with parameters $v_0 = 33m/s$, $T = 1.5s$, $s_0 = 2m$, $a = 0.3m/s^2$, $b = 3m/s^2$ and $\delta = 4$ [19]. Then, $k_p = 0.01$, $k_d = 0.18$ and $k_v = 0.04$.

A. Plant Stability

From (17)-(19), we find that $\epsilon^* = 6.10783$. With $n = 4$, when $\epsilon_i = 0$, Fig. 2a shows that (7) is plant stable, that is, the speed errors converge toward zero. By taking $\epsilon_i \in (0, \epsilon^*)$, system (7) remains plant stable, see Figs. 2b-c. Then it becomes plant unstable when at least one delay becomes bigger than ϵ^* as per Theorem 3.2, see Fig. 2d.

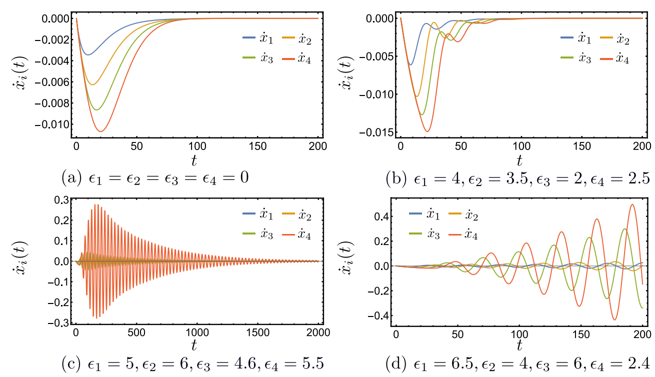

(a) $\epsilon_1 = \epsilon_2 = \epsilon_3 = \epsilon_4 = 0$ (b) $\epsilon_1 = 4, \epsilon_2 = 3.5, \epsilon_3 = 2, \epsilon_4 = 2.5$

(c) $\epsilon_1 = 5, \epsilon_2 = 6, \epsilon_3 = 4.6, \epsilon_4 = 5.5$ (d) $\epsilon_1 = 6.5, \epsilon_2 = 4, \epsilon_3 = 6, \epsilon_4 = 2.4$

Fig. 2. Time series of speed errors $x_i'(t)$ in system (7) with $n = 4$. (a) When there is no delay, the system is plant stable by Lemma 3.2. The critical time delay value is $\epsilon^* = 6.10783$, in (b)-(c) system (7) is plant stable for $(\epsilon_i < \epsilon^*)$ and in (d) system (7) is plant unstable when $(\epsilon_1 > \epsilon^*)$ as per Theorem 3.2.

B. String Stability

In Fig. 3, we plot $|T(j\omega)|^2$ with different time delays. We notice that the range of frequencies $(0, \omega_0)$ becomes bigger as the time delay increases as per Lemma 4.1 and the system in string unstable for $\omega \in (0, \omega_0)$. Usually the largest perturbation in the headway that a vehicle will experience results from lane changing. Typical lane changes occur at headways of $100m$ (in) or $70m$ (out) [1], hence we take a perturbation $\Delta h_{\max}$ to be approximately between $50 - 70m$. When approaching a stalled car or traffic accident from free flow at $v_{\max} = 40m/s$, the maximum rate of change of headway at $\dot{h}_{\max} \approx v_{\max} = 40m/s$. Similarly, when considering accelerating from a dead stop onto an empty highway with free flow speed $v_{\max} = 40m/s$, the maximum velocity difference $\Delta v_{\max} \approx v_{\max} = 40m/s$. Human drivers comfortably accelerate at up to $a_{\max} \approx 0.5\ m/s^2$, with slightly higher tolerance for braking than accelerating [20]. Consequently, we have the upper bounds:

$$k_p \approx \frac{a_{\max}}{\Delta h} < 0.1, \ k_d \approx \frac{a_{\max}}{\dot{h}_{\max}} < 0.2, \ k_v \approx \frac{a_{\max}}{\Delta v_{\max}} < 0.2.$$

This gives an optimal autonomous vehicle controller as $k_{p_R} = 0$, $k_{d_R} = 0.103$ and $k_{v_R} = 0.2$. Choosing $\zeta = k_{v_R}/k_{d_R}$ [1], we plot m^*_{stable} and m^*_{safe} on $(0, \omega_0)$ to find

m^* in Fig. 4. We notice that the time delay has no noticeable effects on m^* when ω is small. However, with time delay, m^* becomes smaller as ω approaches ω_0. Further, in Fig. 5, we observe that when ϵ_H increases, m^* decrease as $\omega \to \omega_0$.

To see the influence of the value of the parameter $p \in \{k_{p_\sigma}, k_{d_\sigma}, k_{v_\sigma}\}$, $\sigma \in \{R, H\}$, on the value of m^*, we take 10% deviation from the value of p in Fig. 4 and plot a heatmap of the corresponding m^* in Figs. 6 and 7. We notice that a small perturbation in these parameters can cause a noticeable change in the value of m^*. In Fig. 8, we plot heatmap of the difference in m^* when decreasing the time delay ϵ_R and ϵ_H in Figs. 6 and 7. We have a similar observation to Fig. 5 where ϵ_H affects the value of m^* more than ϵ_R.

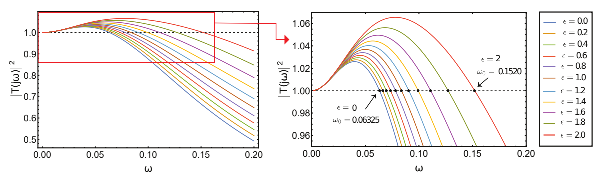

Fig. 3. The influence of time delay on the range of frequencies $(0, \omega_0)$. The time delay is $\epsilon = 0.2k$, $k = 0, \ldots, 10$. We notice the system in string unstable for $\omega \in (0, \omega_0)$.

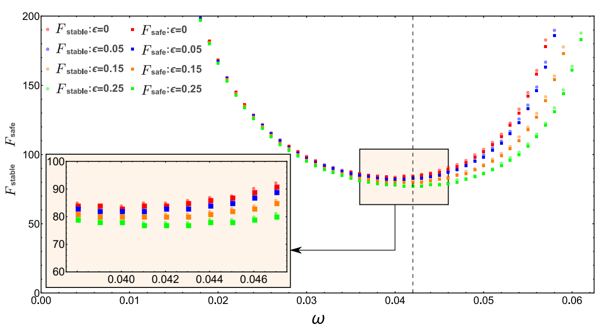

Fig. 4. We vary ω within the unstable region of frequencies (for the HDV) and present the number of vehicles that can be stabilized (○) or safely handled (□) by a single autonomous vehicle with $\epsilon := \epsilon_R = \epsilon_H$. The two curves of F_{stable} and F_{safe} are nearly identical, demonstrating that the optimization procedure successfully chose parameters that optimized for both conditions. The value of m^* is 84 when $\epsilon = 0$, 83 when $\epsilon = 0.05$, 80 when $\epsilon = 0.15$ and 77 when $\epsilon = 0.25$.

VI. Conclusions

We studied a Standard Car Following model with time delays that arise from lags in the input signals to the resulting output acceleration. We used the model to obtain the optimal number of HDVs, denoted as m^*, that can be stabilized using an autonomous vehicle within a single-lane. To this end, we carried out plant stability and string stability analyses to derive string stability and safety conditions. Then, we used these conditions to characterize m^*. Through a numerical study, we found that as the delay increases the value of m^* decreases. For instance, a 0.25 second delay reduced the value of m^* from 84 vehicles to 77 vehicles. We also found that the effects of the time delay in the autonomous vehicle was not as remarkable as the time delay in the human-driven vehicles on m^*. Future research will consider

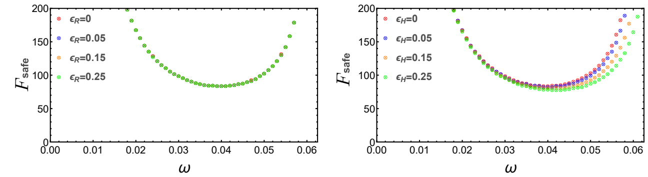

(a) $\epsilon_H = 0.01$ (b) $\epsilon_R = 0.01$

(c) $\omega = 0.02$ (d) $\omega = 0.05$

Fig. 5. The effect of ϵ_R and ϵ_H on the number of human vehicles a single autonomous vehicle can safely and efficiently stabilize. As ω approaches ω_0, we observe that ϵ_H affects the number of cars while ϵ_R has no noticeable effects.

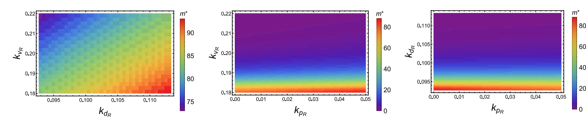

Fig. 6. Heatmap of the number m^* with 10% deviation from the value of $\{k_{p_R}, k_{d_R}, k_{v_R}\}$ in Fig. 4. The parameters $\{k_{p_H}, k_{d_H}, k_{v_H}\}$ are similar to those in Fig. 4 with $\epsilon = 0.15$ and $\omega = 0.0425$. A small perturbation in the autonomous vehicle parameters is sufficient to cause a change in the value of m^*.

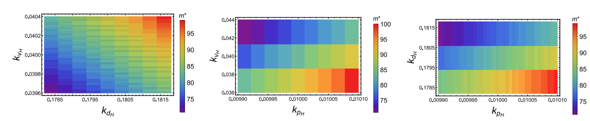

Fig. 7. Heatmap of the number m^* with 10% deviation from the value of $\{k_{p_H}, k_{d_H}, k_{v_H}\}$ in Fig. 4. The parameters $\{k_{p_R}, k_{d_R}, k_{v_R}\}$ are similar to those in Fig. 4 with $\epsilon = 0.15$ and $\omega = 0.0425$. A small perturbation in the HDVs parameters is sufficient to cause a change in the value of m^*.

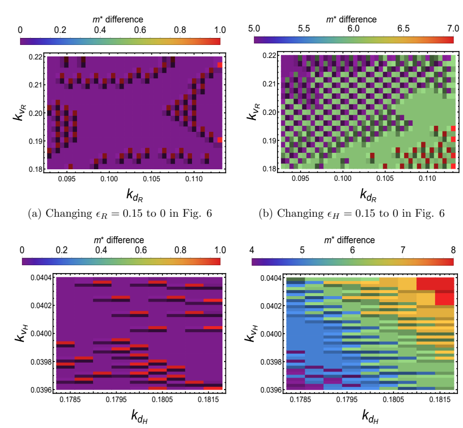

(a) Changing $\epsilon_R = 0.15$ to 0 in Fig. 6 (b) Changing $\epsilon_H = 0.15$ to 0 in Fig. 6

(c) Changing $\epsilon_R = 0.15$ to 0 in Fig. 7 (d) Changing $\epsilon_H = 0.15$ to 0 in Fig. 7

Fig. 8. Heatmap of the difference in m^* when changing the time delay to 0 in Figs. 6 and 7. The simulation results of this figure show that the time delay in HDVs ϵ_H affects m^*, while ϵ_R does not affect m^*.

the platoon (connected autonomous vehicles network) to stabilize human-driven vehicles.

REFERENCES

[1] C. Wu, A. Bayen, and A. Mehta, "Stabilizing traffic with autonomous vehicles," in *IEEE International Conference on Robotics and Automation (ICRA)*, pp. 6012–6018, 2018.

[2] Y. Sugiyama, M. Fukui, M. Kikuchi, K. Hasebe, A. Nakayama, K. Nishinari, S.-i. Tadaki, and S. Yukawa, "Traffic jams without bottlenecks—experimental evidence for the physical mechanism of the formation of a jam," *New Journal of Physics*, vol. 10, no. 3, pp. 1–7, 2008.

[3] D. Swaroop, *String stability of interconnected systems: An application to platooning in automated highway systems*. California Partners for Advanced Transit and Highways, 1997.

[4] V. Milanés and S. E. Shladover, "Modeling cooperative and autonomous adaptive cruise control dynamic responses using experimental data," *Transportation Research Part C: Emerging Technologies*, vol. 48, pp. 285–300, 2014.

[5] R. Stern, S. Cui, M. Delle Monache, R. Bhadani, M. Bunting, M. Churchill, N. Hamilton, H. Pohlmann, F. Wu, B. Piccoli, *et al.*, "Dissipation of stop-and-go waves via control of autonomous vehicles: Field experiments," *Transportation Research Part C: Emerging Technologies*, vol. 89, pp. 205–221, 2018.

[6] V. Giammarino, S. Baldi, P. Frasca, and M. Delle Monache, "Traffic flow on a ring with a single autonomous vehicle: An interconnected stability perspective," *IEEE Transactions on Intelligent Transportation Systems*, 2020.

[7] A. Kreidieh, C. Wu, and A. Bayen, "Dissipating stop-and-go waves in closed and open networks via deep reinforcement learning," in *International Conference on Intelligent Transportation Systems (ITSC)*, pp. 1475–1480, 2018.

[8] V. Kurtc and I. Anufriev, "Car-following model with explicit reaction-time delay: linear stability analysis of a uniform solution on a ring," *Mathematical Models and Computer Simulations*, vol. 9, no. 6, pp. 679–687, 2017.

[9] W. Qin and G. Orosz, "Experimental validation of string stability for connected vehicles subject to information delay," *IEEE Transactions on Control Systems Technology*, vol. 28, no. 4, pp. 1203–1217, 2019.

[10] W. Qin and G. Orosz, "Scalable stability analysis on large connected vehicle systems subject to stochastic communication delays," *Transportation Research Part C: Emerging Technologies*, vol. 83, pp. 39–60, 2017.

[11] M. Bando, K. Hasebe, A. Nakayama, A. Shibata, and Y. Sugiyama, "Dynamical model of traffic congestion and numerical simulation," *Physical Review E*, vol. 51, no. 2, pp. 1035–1042, 1995.

[12] M. Treiber, A. Hennecke, and D. Helbing, "Congested traffic states in empirical observations and microscopic simulations," *Physical Review E*, vol. 62, no. 2, pp. 1805–1824, 2000.

[13] G. Orosz and S. P. Shah, "A nonlinear modeling framework for autonomous cruise control," in *Dynamic Systems and Control Conference (DSCC)*, vol. 45301, pp. 467–471, 2012.

[14] D. Bernstein, *Matrix mathematics: theory, facts and formulas*. Princeton university press, 2009.

[15] W. Levine, *The Control Handbook (three volume set)*. CRC press, 2018.

[16] S. Cui, B. Seibold, R. Stern, and D. Work, "Stabilizing traffic flow via a single autonomous vehicle: Possibilities and limitations," in *IEEE Intelligent Vehicles Symposium (IV)*, pp. 1336–1341, 2017.

[17] D. Swaroop and K. Hedrick, "String stability of interconnected systems," *IEEE Transactions on Automatic Control*, vol. 41, no. 3, pp. 349–357, 1996.

[18] S. Hu, H. Wen, L. Xu, and H. Fu, "Stability of platoon of adaptive cruise control vehicles with time delay," *Transportation Letters*, vol. 11, no. 9, pp. 506–515, 2019.

[19] M. Treiber and A. Kesting, "Car-following models based on driving strategies," in *Traffic Flow Dynamics*, pp. 181–204, 2013.

[20] L. Hoberock, "A survey of longitudinal acceleration comfort studies in ground transportation vehicles," tech. rep., Council for Advanced Transportation Studies, 1976.